

Theory of vertical and lateral Stark shifts of excitons in quantum dots

M. Sabathil^{*1}, S. Hackenbuchner, S. Birner, J. A. Majewski, P. Vogl, J. J. Finley

The shape and alloy composition of self-assembled InGaAs quantum dots that are buried beneath a cap layer of GaAs is currently of great interest but still poorly understood. There are several direct experimental methods such as STM, TEM, or x-ray diffraction that provide some information about the composition of the quantum dots. However, all of these techniques have the drawback of either being destructive or being limited to dots on the surface that differ from buried quantum dots (QD). By contrast, the recent development of single dot spectroscopy allows one to examine the optical properties of individual quantum dots under the influence of external perturbations such as electric or magnetic fields. The dependence of the optical and electronic properties on these external fields provides an important albeit indirect probe of the shape and alloy composition of the quantum dot. This situation calls for the development of a reliable, quantitative theoretical model for the electronic properties of QD of any given shape and alloy profile, in order to be able to link measured exciton energies or relative transition intensities of single QD with their shape and composition.

In this work we present systematic predictions of the bias dependence of the electronic structure of self-assembled quantum dots for a wide variety of dot shapes, alloy profiles and show that the combined effect of applied and (piezoelectric) internal electric fields yields detailed information about shape and composition profiles. We therefore chose a multiband- $\mathbf{k}\cdot\mathbf{p}$ Schrödinger-Poisson approach that takes into account the Coulomb interaction between confined electrons and holes, as well as the applied and induced piezoelectric fields fully self-consistently. The present calculations have been carried out with the device simulator `nextnano`³. Based on single particle eigenstates obtained from the solution of an 8-band $\mathbf{k}\cdot\mathbf{p}$ Hamiltonian, the exciton energy is calculated self-consistently within the Hartree approximation.

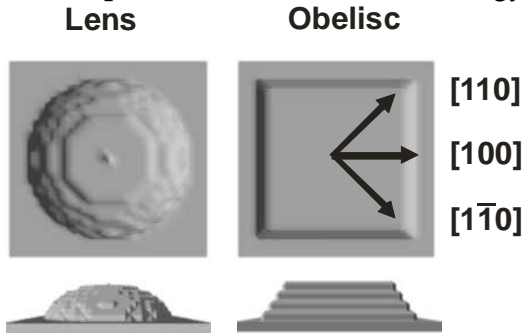


Fig. 1. The two types of quantum dot shapes considered in this work: lens and obelisk shapes. The height and base width of these dots are varied between 3 to 5 and 15 to 25 nm respectively. The directions of the lateral electric fields that are taken into account are indicated.

Assuming a separable exciton wave function, the Coulomb interaction between electron and hole is calculated by iteratively solving the Poisson and Schrödinger equation for each particle, taking into account external and internal potentials including image charges due to the variation of the dielectric constant. The equations are solved within a finite differences scheme on an inhomogeneous grid with 1 nm grid spacing inside the quantum dot resulting in about 3×10^5 grid points. The strain is calculated by minimizing the total elastic energy, including the wetting layer and a sufficiently large GaAs substrate and cap volumes, in order to minimize artefacts from boundaries. The resulting strain-

¹phone:+49-89-289-12762, email: sabathil@wsi.tum.de

induced band deformations and piezoelectric charges are fully taken into account in the above self-consistent cycle. In this way we have calculated exciton transition energies for various In(Ga)As dot shapes and alloy profiles under the influence of vertically and laterally applied electric fields.

The simulated structure consists of a 20 nm thick GaAs substrate, a 1 nm wetting layer with an Indium content of 50 % and the quantum dot with an In concentration that varies from 50 % to 100 %. The dot is capped by a GaAs layer. We have examined two classes of QD shapes that have been discussed in the literature, lens-shaped and truncated pyramidal ("obelisk") dots namely [Fig. 1]. The height of the QD has been systematically varied from 3 to 5 nm and the base width from 15 to 25 nm, respectively. These values lie within the range of experimentally estimated dot sizes. In addition, we considered two types of alloy profiles, a simple linear and an angular profile. In the latter case, the Indium concentration varies with the polar angle relative to the center axis of the dot [Fig. 2]. This profile is supported by STM measurements and by theoretical models of the growth process and leads to an inverted pyramid of high Indium content inside the quantum dot. The most important feature of this alloy profile is the fact that it produces a vertical and a lateral variation of the Indium concentration which has been neglected so far.

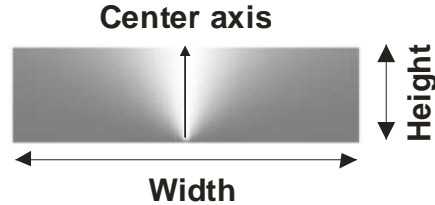


Fig. 2. The angular alloy profile where the Indium concentration depends on the polar angle relative to the center axis of the QD. Light and dark grey-scale indicates high and low In content, respectively.

The polarizability of the exciton in a lateral electric field is sensitive measure of the alloy profile of the quantum dot that depends particularly on the base width of the QD [Fig. 3]. In the case of the vertically linear alloy profile, one has a laterally homogeneous Indium concentration. Not surprisingly, this yields a very large polarizability for both types of QD shapes. The radial alloy profile, on the other hand, leads to an inverted pyramid of Indium content in the QD that in turn gives a strong lateral confinement of the hole. This effect reduces the polarizability drastically, typically by a factor of two compared to the linear alloy profile. Therefore, the alloy profile can be determined once the width of the quantum dot is known. The dots with a radial profile show a base width dependence of the polarizability that is very similar for both types of QD shapes. By contrast, QD with a laterally homogeneous profile possess a strong width dependence of the polarizability when they are obelisk-shaped but a weak one in the lens-shaped case. This is due to the fact that the curved surface of the lens QD enhances the lateral confinement which in turn limits the polarizability.

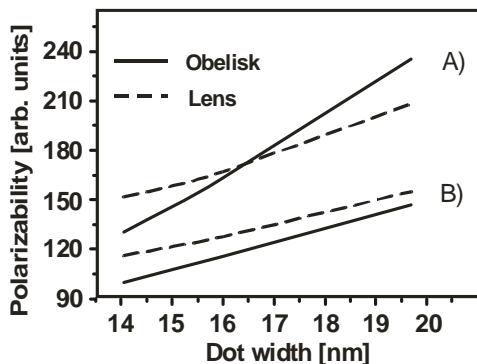


Fig. 3. Predicted lateral polarizability shown as a function of the base width of the quantum dot for different shapes and alloy profiles. The polarizability is much larger for dots (A) with a laterally homogeneous alloy profile than for (B) dots with a radial profile since the latter provides a strong lateral confinement for the hole. For both alloy profiles, the results are shown for obelisk-shaped (full lines) as well as for lens-shaped quantum dots (dashed lines).